Source- vs topographic-forcing in pyroclastic currents: the case of the Orvieto-Bagnoregio Ignimbrite, Vulsini, central Italy

Danilo M. Palladino [*], Mauro Pettini

Department of Earth Sciences, "Sapienza" University of Rome, Rome, Italy

ARTICLE INFO

ABSTRACT

The main pyroclastic flow unit of the Orvieto-Bagnoregio Ignimbrite (Vulsini, central Italy) provides a striking example of increasing thickness with distance from the vent, accompanied by opposite size-distance trends for lithic and juvenile clasts. Lithic clasts show normal lateral grading, while dense (1120-1400 kg/m^3) scoria clasts show inverse lateral grading. The latter trends are attributed to the opposite density contrast with respect to the flow medium of gas and fine particles and put a constraint to the minimum density of the transporting flow. Thus, the study example approaches the high concentration, non-turbulent end-member of pyroclastic currents. By applying the topological aspect ratio approach, we infer a forced behavior of the parent flow in proximal to intermediate settings, due to sustained feeding with high mass discharge rate at source. In distal settings, the source-forced regime was enhanced by topographic forcing due to channeling along radial topographic lows, thus resulting in increasing bulk density and runout of the current. By analogy with the mobility of dry debris flows, the sliding component of transport prevailed from proximal to intermediate settings, accounting for the prevailing tendency of the pyroclastic current to transport than to deposit, thus forming a relatively thin deposit with normal lateral grading of lithics. The spreading component dominated toward the distal settings, resulting in increasing pyroclast accumulation (up to tens of meters of thickness) and delayed deposition of coarsest scoria clasts as far as the final runout.

Keywords: pyroclastic current; ignimbrite; flow regime; thickness; clast size; Vulsini.

INTRODUCTION

Pyroclastic currents are defined as gravity-driven, ground-hugging, gas-pyroclast mixtures produced during explosive volcanic eruptions, and comprise a full spectrum of particle concentrations, flow regimes and particle support mechanisms (e.g., Druitt, 1998; Sulpizio et al., 2014; Bonadonna et al., 2016; Palladino, 2017 and reference therein). They rank among the most hazardous manifestations of geologic activity on Earth, as they can transport considerable amounts of mass and energy at great distance from their source and impact severely the human communities. Thus, defining the areas exposed to their effects (mostly in terms of dynamic pressure and heat) is a crucial issue of modern volcanology.

Given the very complex nature and the very limited possibility of direct observation, the fluid-dynamic characterization of pyroclastic currents largely bears on field aspects and laboratory analyses of the deposits from past eruptions, in light of theoretical studies and analogue modeling (e.g., Valentine, 1987, 1998; Palladino and Valentine, 1995; Druitt, 1998; Branney and Kokelaar, 2002; Dellino et al., 2007; Sulpizio et al., 2014, and

PM

reference therein). The mobility, dispersal pattern and total runout of pyroclastic currents essentially depend on the eruptive parameters at source (i.e., grain size and component characteristics of the erupting mixture, mass discharge rate, fountaining height, duration, etc.), as well as on the interactions with the surroundings (topography, atmosphere, hydrosphere) along their path (e.g., Fisher et al., 1993; Dufek et al., 2009; Andrews and Manga, 2011; Fauria et al., 2016; Giordano and Doronzo, 2017; Valentine et al., 2019). However, despite theoretical advances from countless studies, linking unambiguously the field aspects of deposits to the key characteristics of the parent pyroclastic currents and their emplacement dynamics is still challenging.

In light of the proposed characterization of the flow regime in terms of "forced convection-dominated" vs "inertia-dominated" end members (Doronzo, 2012), Giordano and Doronzo (2017) used a field-based approach to evaluate the relative roles of transport vs sedimentation along the flow path of a pyroclastic current. Based on a re-appraisal of the deposit aspect ratio concept (i.e., the ratio of the average thickness of the deposit to its horizontal extent; Walker et al., 1980, Walker, 1983), Giordano and Doronzo (2017) introduced a "Topological Aspect Ratio" (AR_t; see definition in the Methods) and its gradient downcurrent to define the forced vs inertial regime as a function of the flow runout (distance travelled from the source) and topography.

More recently, Palladino and Giordano (2019) tested this approach on a selected pair of pyroclastic units of the Latera Volcano (in the western part of the Vulsini Volcanic District, central Italy), as representative of the two end members of the "classical" spectrum of pyroclastic currents in terms of high vs low particle concentration and laminar vs turbulent flow regime. In this case, peculiar deposit thickness and clast size trends with distance from source provided mutually consistent inferences to constrain the different types of pyroclastic currents. This type of studies makes it possible to establish a link among the deposit characteristics measurable in the field (i.e., thickness and maximum clast sizes) and the relevant physical properties that control the dynamics and mobility of the parent pyroclastic currents (subject to significant changes along flow path) and, ultimately, to evaluate the relative roles of source vs local topography parameters in controlling the final runout. Here, we apply the same approach to the main pyroclastic flow unit of the Orvieto-Bagnoregio ignimbrite (WOB), in the north-eastern part of Vulsini. Our observations extend the spectrum of available field examples, aiming at defining the reference end-member patterns for future applications to other cases elsewhere.

GEOLOGICAL SETTING

The Vulsini Volcanic District is part of the Quaternary potassic Roman Province (central Italy; Figure 1). The Vulsini volcanic activity, spanning ca. 0.6-0.1 Ma, is attributed to five volcanic complexes or lithosomes (Palladino et al., 2010 and reference therein), i.e.: Paleovulsini, Vulsini Fields, Latera, Montefiascone and Bolsena-Orvieto. The latter developed in the NE sector of the district and was the source of the Orvieto-Bagnoregio ignimbrite (WOB), which we focus on in this paper, regarded as a major caldera-forming explosive event in the NE portion of the polygenetic Bolsena Caldera (Nappi et al., 1994; Acocella et al., 2012; Palladino et al., 2014). The WOB eruption age of 333.0±3.8 ka (Nappi et al., 1995) is fully consistent with a new radiometric dating at 332.5±1.4 ka (Marra et al., 2019).

The WOB eruption products crop out over an area of approx. 150 km², NE of Lake Bolsena, as far as the Tiber River valley (Figure 2), with an estimated volume in the order of a few km³. In most proximal settings, around Bolsena town, the WOB eruptive succession comprises, from base to top (Figure 3): i) a few decimeter-thick, well-sorted horizon of whitish-light gray, sub-aphyric (sanidine-bearing) pumice lapilli, from Subplinian fallout (Orvieto-Bagnoregio pumices, P3; Nappi et al., 1994). Isopach and isopleth data indicate a source vent near the present NE shore of Lake Bolsena, deposit volume of 0.2 km³ (0.07 km³ DRE), maximum column height of 16 km and corresponding peak mass discharge rate of 2×10^7 kg/s (Nappi et al., 1994); ii) a few meter-thick, poorly consolidated, lithic-rich ash-pumice flow deposit (overlying a distinctive few centimeter-thick ground surge layer), intimately associated with lenses of coarse-grained, fines-poor, "co-ignimbrite lag breccia" (Walker, 1985), identified as a typical example of proximal facies that marks the onset of caldera collapse. Leucite (turned to analcime)-bearing, moderately vesicular, dark gray-black scoria and spatter blocks also occur toward the top.

In intermediate and distal settings (e.g., Bagnoregio-Lubriano, Orvieto; Figure 2), on top of the basal fallout horizon (which thins to a few centimeters) is the occurrence of multiple, decimeter-thick, matrix-supported, inversely graded flow divisions, with tractional features (Capaccioni and Sarocchi, 1996; "type 2" pyroclastic currents; Palladino and Simei, 2002), containing whitish-light grey, crystal-poor, sanidine-bearing, pumice lapilli. Upsection, the main pyroclastic flow deposit (the most distinctive of WOB eruption) is made up of a reddish tuff, lithified due to zeolitization process, a few meter- up to tens of meter-thick, enclosing porphyritic (sanidine+leucite-bearing), moderately vesicular, black scoria clasts (Figure 3).

Juvenile pumice and scoria clasts plot in the trachyte and phonolite fields of the TAS diagram (Nappi et al.,
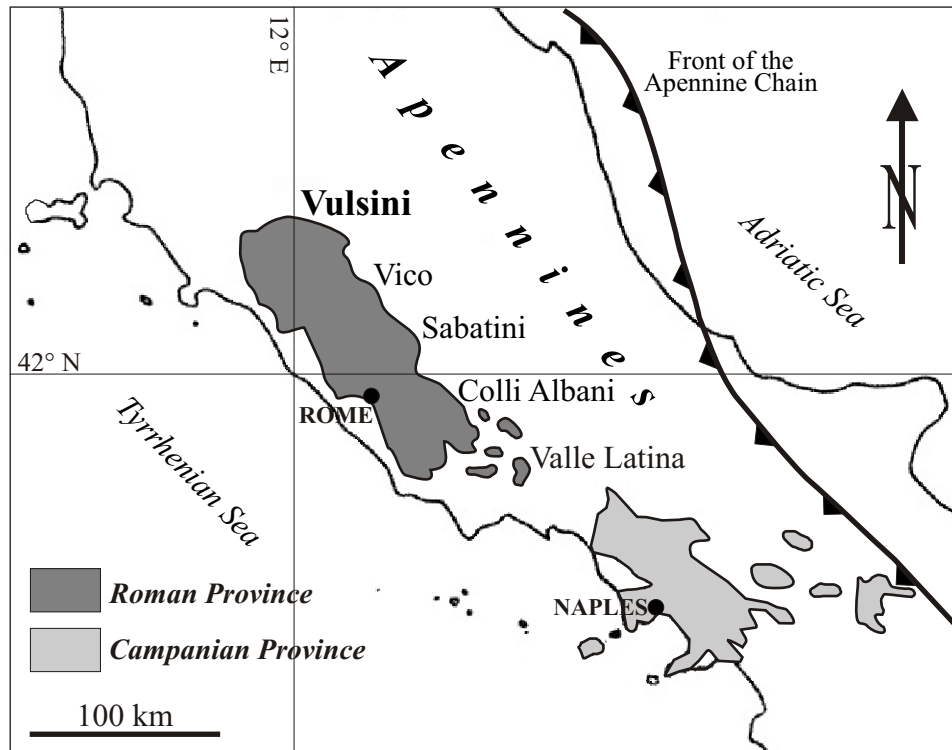
Figure 1. Sketch map of the Quaternary volcanic districts of the Roman and Campanian provinces (central Italy), showing the location of the Vulsini Volcanic District (after Palladino et al., 2010).

Figure 2. Sketch location map of the measured outcrops (red crosses) and areal distribution (dashed line) of the WOB main pyroclastic flow unit. The two flow paths (i.e., Path 1: Bolsena-Lubriano and Path 2: Bolsena-Orvieto), which deposit thickness data are referred to in Figure 4 are also shown.

1994; Palladino et al., 2014). According to Palladino et al. (2014), the observed textural and compositional changes in the juvenile component upsection consistently indicate a shift from a central conduit (feeding the Suplinian phase) to a ring-fault system, concomitant to caldera collapse, feeding the lithic-rich lag breccia and the associated black scoria-bearing pyroclastic flow deposit.

Here, we report on thickness and maximum clast size variations occurring in the WOB main pyroclastic flow unit, to define the dynamics of the parent pyroclastic current in response to the distance travelled from the source vent and ground topography.

Figure 3. Field aspects of WOB (outcrop localities in Table 1): a) Bolsena, Madonna del Giglio locality; proximal exposure of the coarse lithic-rich lag breccia, overlying the co-eruptive Subplinian pumice fall horizon. Here, WOB deposits are cut by a normal fault (scale: bar divisions 10 cm); b) the medieval village of Civita di Bagnoregio is built on an isolated rock cap of WOB red tuff, overlying a stratified pyroclastic succession from previous explosive activity of Bolsena-Orvieto and Paleovulsini volcanic complexes; c) Rocca di Ripesena locality; close-up of the lithified red tuff with leucite-bearing black scoria clasts, the most typical lithofacies of the WOB main pyroclastic flow unit (black scoria in the centre is 20 cm-sized).

METHODS

Thickness measurements were performed in all available exposures of the WOB main pyroclastic flow unit, to define the variation trend of the deposit thickness with distance from the inferred source vent, broadly corresponding to the present-day Bolsena town area. Maximum lithic and pumice clast sizes (ML5 and MP5, respectively) were determined at each exposure by taking the average of the long axis of the five largest clasts in a 2 m width x 1 m height area, both in the lower and upper halves of the main pyroclastic flow deposit. Thickness and clast size data present uncertainties in a few, partially inaccessible, exposures (such as high tuff cliffs; e.g. Lubriano), where measurements were made indirectly from distance based on photographs with a reference scale.

Following Giordano and Doronzo (2017), as well as the application in Palladino and Giordano (2019), we used the "Topological Aspect Ratio" (AR_t) as a proxy to describe the interplay between sedimentation and mobility of the parent pyroclastic current. For each outcrop, we calculated the AR_t value as the ratio of the local deposit thickness (Ht, in meters) to the potential runout (Lt, in kilometers), which is the distance between the local site and the maximum runout distance (thus Lt varies between the maximum value at the vent and 0 at the maximum runout distance). For a pyroclastic current at a given locality, Ht represents its tendency to deposit and Lt its tendency to transport pyroclastic material further downcurrent, i.e. its mobility. Therefore, an increasing AR_t downcurrent along a given flow path (i.e. positive $d(AR_t)/dx$, with constant or even increasing thickness with distance) vs a decreasing AR_t downcurrent (i.e., negative spatial gradient $d(AR_t)/$

dx) would discriminate respectively between forced vs inertial flow regime of the parent current. A flat AR_t gradient (i.e. mildly decreasing thickness with nearly constant AR_t) would indicate a balance between the two regimes (Doronzo, 2012; Giordano and Doronzo, 2017; Palladino and Giordano, 2019).

In addition, from the maximum clast size trends with distance from source, we derived the "Competence Ratio" (CR) and its gradient d(CR)/dx, as a measure of the ability of the pyroclastic current to support pyroclasts downcurrent (Palladino and Giordano, 2019). At a given locality, CRl and CRp (for lithic and pumice clasts, respectively) are defined by the ratio of the local maximum clast size (ML5 and MP5) to the potential runout (Lt), i.e., again, the distance left from the final runout. The comparison of the CRl, CRp and AR_t trends provide key inferences for transport and depositional dynamics (Palladino and Giordano, 2019).

Due to uncertainty in the location of the source vent of the pyroclastic current, we considered the reference distance "zero" as the most proximal outcrop (near Bolsena town; Figure 2), where the occurrence of the lag breccia likely indicates a close proximity to a feeder ring fault segment of the collapsing caldera. Due to the uncertainty in evaluating the maximum distance travelled by the pyroclastic current, the final runout was chosen based on the most distal available exposure, by adding arbitrarily 1 km to avoid Lt values <1 km in the calculations of AR_t and CR.

Finally, in selected outcrops, we performed field-scale modal analysis, by means of a grid of one square meter divided into meshes of 5 cm per grid side, obtained by marking the cross-points on a transparent sheet, resulting in a total of 400 points. This was then pinned with nails on the rock face, and used to count the amounts of different components, such as pumice and lithic clasts, ash matrix and free crystals. In addition, pumice clast densities in different size fractions were determined by water displacement method, by wrapping (after weighting) pumice clasts with an aluminum foil before being immersed in a known volume of water.

RESULTS

Measured deposit thickness and maximum lithic and pumice/scoria clast sizes for the WOB main pyroclastic flow unit are reported in Table 1, as a function of the distance travelled. In addition, thickness data are shown in Figure 4, also split in two different radial flow paths (i.e., Path 1: Bolsena-Lubriano and Path 2: Bolsena-Orvieto; Figure 2). Quite strikingly, in both cases, the deposit thickness reaches its maximum values at the most distal exposures, i.e. respectively, at Lubriano (22.5 m, 10 km from the inferred source) and at Orvieto and surroundings

(Bardano, Rocca Ripesena; 16-21 m, 12-13.5 km away from source).

Thickness trends are best fitted by an exponential law, highlighting an overall marked increase of thickness with distance from the vent. This appears as a first-order general tendency that holds at the scale of the whole flow runout, beyond some scatter related to thickness variations transverse to the general radial flow path due to local topographic effects. Indeed, flow channeling along radial (ENE-oriented) paleovalleys is particularly evident in the area of Civita di Bagnoregio and Lubriano (distal end of the radial flow path 1), where the WOB main pyroclastic flow unit (i.e., the red tuff with black scoria) varies in thickness considerably in response to the depositional surface (i.e., it thickens along radial topographic lows and thins on topographic highs), maintaining a flat top, slightly inclined downcurrent toward the Tiber River valley. WOB exposures 2 km ENE (downcurrent) of Civita di Bagnoregio show the occurrence of the basal pumice fall horizon overlain by multiple thin ashy-pumiceous units, while the main red tuff with black scoria is completely lacking and is not found further downcurrent. Thus, we are confident that the maximum thickness was actually achieved toward the final runout distance and that the latter was not determined by a possible blocking of the flow due to transverse topographic barriers (actually lacking), yet by intrinsic flow properties (see following section).

Overall, in Table 1 and Figure 5, we observe an increase of AR_t with distance from vent (best fitted by a power-law relationship), i.e. a slightly increasing AR_t from proximal to intermediate locations, followed by an abrupt increase toward the distal reaches (L_t <6 km).

The maximum lithic and pumice/scoria clast sizes show opposite trends with distance from the inferred vent (Figure 6): lithic sizes show an exponential decrease from proximal to distal locations (ML5 values decrease from 24 cm to 1 cm), whereas pumice and scoria sizes increase exponentially (MP5 values increase from 2-3 cm to >20 cm). Moreover, in relatively distal settings, decimeter-sized dark scoria clasts tend to concentrate toward the top of the deposit and are usually coarser than associated light grey pumice clasts in the lower part of the flow unit. Measured densities range 620-650 kg/m^3 for highly vesicular, light grey pumice lapilli (determined in the 1-4 cm size fraction), and 1120-1400 kg/m^3 for dark scoria clasts (in the 6-12 cm size fraction).

CR values for lithic and pumice/scoria clasts, determined following Palladino and Giordano (2019), are reported in Table 1 and Figure 7. Lithic clasts, beyond the abrupt decrease of CRl values observed in the proximal setting (i.e., Lt between 14 and 10 km), show a relatively constant CRl. We note that this break in slope in the CRl-distance

Table 1. List of measured outcrops, reporting thickness and maximum clast size data and related parameters (see text for definitions) for the WOB main pyroclastic flow unit. Asterisks mark the occurrence of co-ignimbrite lag breccia.

Locality	Latitude N, longitude E	Distance (km)	Potential runout Lt (km)	Thickness Ht (m)	ML5 (cm)	MP5 lower/ upper (cm)	ARt	CRl	CRp lower/upper
Bolsena-Santa Cristina (*)	42,544287 11,896311	0.0	14.5	6.0	24.0	3.8	0.41	1.66	0.26
Road Bolsena-Madonna del Giglio (*)	42,484389 11,599318	0.2	14.3	3.2	16.0	2.8	0.22	1.12	0.20
Madonna del Giglio (*)	42,434125 11,501138	0.6	13.9	2.2	12.5		0.16	0.90	
Capraccia	42,631115 12,044506	4.5	10.0	1.8	3.6	2.1	0.18	0.36	0.21
Torre di San Severo	42,671114 12,062361	7.8	6.7	4.5	2.1	12.9	0.67	0.31	1.93
Bagnoregio-cemetery	42,624919 12,084175	8.2	6.3	5.2	2.4	13.2	0.83	0.38	2.06
Bagnoregio	42,625945 12,085342	9.0	5.5	8.0	1.9	13.1/14.8	1.45	0.35	2.38/2.69
Bagnoregio-Belvedere	42,625403 12,106047	9.3	5.2	11.0	2.3	14.4/15.6	2.12	0.44	2.77/3.00
Road Bagnoregio-Lubriano	42,633468 12,092212	9.5	5.0	8.7	2.0	16.8/17.1	1.74	0.40	3.36/3.42
Civita di Bagnoregio	42,626054 12,108564	9.7	4.8	19.5	2.1	14.6	4.06	0.44	3.04
Lubriano cliff	42,636028 12,110326	10.0	4.5	22.5	2.2	22.3/22.1	5.00	0.49	4.96/4.91
Canonica	42,705887 12,077564	10.5	4.0	14.2	2.0	19.8/18.5	3.55	0.50	4.95/4.63
Lubriano	42,636978 12,110415	10.6	3.9	16.9			4.33		
Sugano	42,709815 12,053301	10.7	3.8	14.5	1.7	19.5	3.82	0.45	5.13
Porano	42,687174 12,095949	10.8	3.7	>7.6	1.2	8.7	>2.05	0.32	2.35
Orvieto-Fontana del Leone	42,714512 12,112134	11.8	2.7	19.8	1.1	11.2/16.3	7.33	0.41	4.15/6.04
Orvieto cliff-Cathedral	42,717141 12,118333	12.7	1.8	16.3	0.9	13.7/15.8	9.06	0.50	7.61/8.78
Orvieto cliff-central	42,720759 12,108473	12.9	1.6	17.3	1.2	14.3/16.4	10.81	0.75	8.94/10.25
Rocca di Ripesena	42,722321 12,067842	13.3	1.2	21.0	1.1	16.5/17.0	17.50	0.91	13.75/14.20
Bardano	42,750112 12,056021	13.5	1.0	16.5	1.1	14.9	16.50	1.10	14.90

trend parallels a change in the mechanisms for lithic support and sedimentation passing from the near-vent lag breccia to the associated pyroclastic flow downcurrent. The CRl increase in the most distal locations (Lt <2 km) is a mere consequence of the small size (ML5=1 cm) of transported lithics irrespective of distance. Conversely, CRp values increase markedly downcurrent with an exponential trend.

In Table 2 we report field-scale componentry in terms of modal percentages of ash matrix, pumice/scoria, lithics, and free crystals. Besides the occurrence of a coarse lithic-rich lithofacies at the most proximal location (i.e., co-ignimbrite lag breccia, at Bolsena-Santa Cristina), the other measured exposures do not show significant changes in componentry with distance. For instance, the amount of ash matrix in the <1 mm fraction remains
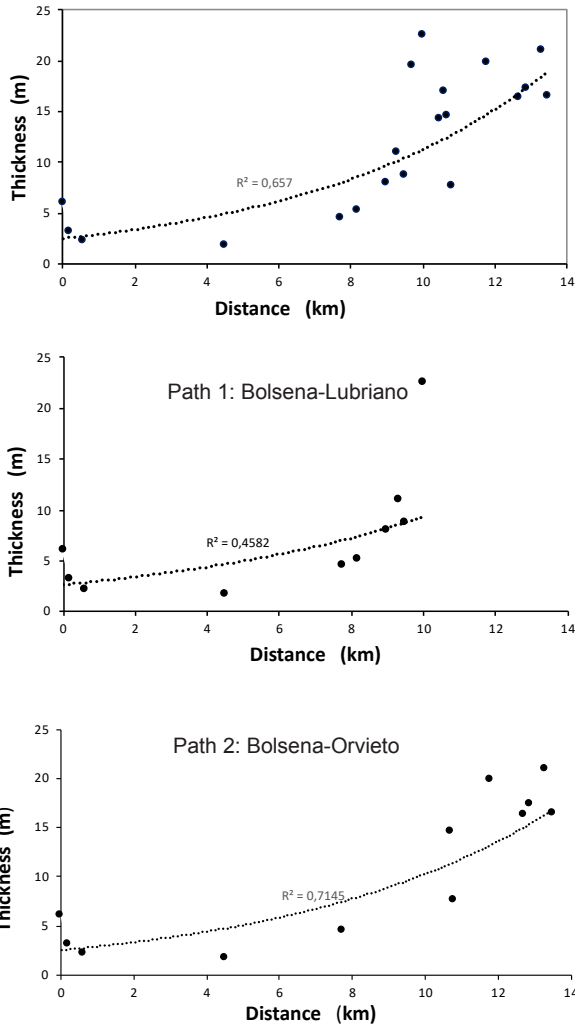
Figure 4. Plots of deposit thickness vs distance from the inferred vent for the WOB main pyroclastic flow unit: all measured localities (top); Bolsena-Lubriano radial path (middle); Bolsena-Orvieto radial path (bottom). Thickness data from Table 1; radial paths are shown in Figure 2. Note the exponential trends of increasing thickness with distance.

Figure 5. Plot of the AR_t values vs the potential runout L_t (see text for definitions) for the WOB main pyroclastic flow unit. The increasing AR_t values with distance from vent indicates a "forced" behavior of the parent current.

Figure 6. Plots of maximum lithic clast sizes (ML5; a) and maximum juvenile clast sizes (MP5; b) vs distance from vent. In some cases, MP5 was measured both in the lower half (mostly pumice clasts, open circles) and in the upper half (black scoria clasts, black circles) of the pyroclastic flow deposit. Maximum clast size data from Table 1. Note the opposite size-distance trends for lithic and juvenile clasts. See methods for definition of ML5 and MP5.

approximately constant at 50%. The slight increase of free crystals towards the most distal locations might be the widely recognized effect of the progressive elutriation of fine vitric particles along flow path to form an overriding co-ignimbrite ash cloud (Sparks and Walker, 1977).

DISCUSSION AND CONCLUSIONS

The WOB main pyroclastic flow unit provides a striking example of increasing thickness with distance from the eruptive source, accompanied by normal and inverse lateral coarse-tail grading for lithic and juvenile clasts, respectively. This particular grading pattern, consistent
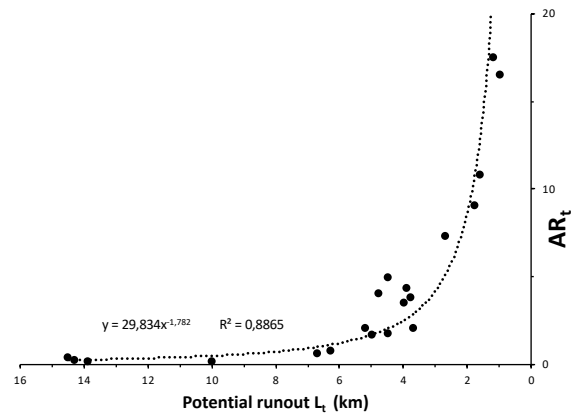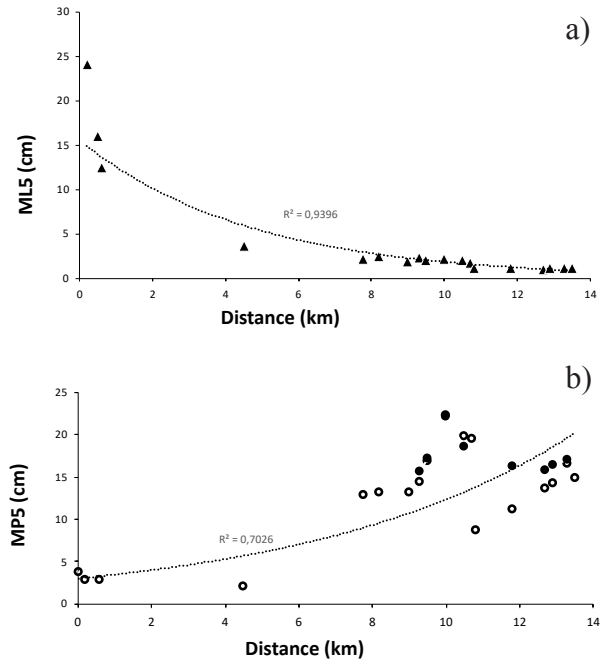
Table 2. Componentry of the WOB main pyroclastic flow unit, expressed as point percentages from field-scale modal analysis (see text for methods). Asterisk marks the occurrence of co-ignimbrite lag breccia.

| Locality	Distance (km)	Ash matrix %	Juvenile pumice/ scoria clasts %	Lithic clasts %	Free crystals %
Bolsena-Santa Cristina (*)	0.01	28.0	32.0	38.0	2.0
Torre di San Severo	7.75	52.0	29.5	11.5	7.0
Bagnoregio-cemetery	8.20	51.4	31.7	7.9	4.0
Bagnoregio	9.00	52.3	31.5	9.0	6.2
Bagnoregio-Belvedere	9.30	53.0	30.0	12.5	4.5
Civita di Bagnoregio	9.60	58.0	26.0	10.7	5.3
Lubriano	10.00	49.0	34.5	7.0	9.5
Orvieto-Fontana del Leone	11.80	52.9	33.2	5.8	8.1
Orvieto cliff-Cathedral	12.70	53.3	29.2	6.2	11.3
Orvieto cliff-central	12.90	52.0	33.8	5.2	9.0
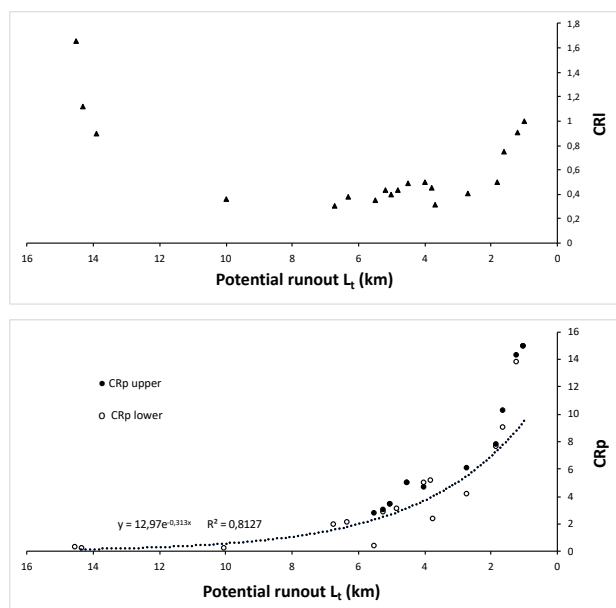
Figure 7. Plots of CR values for lithic (CRl; top) and pumice/scoria (CRp; bottom) clasts vs distance from vent (see text for definition of CR; maximum clast size data from Table 1).

with the constancy of componentry with distance, is an indication of a high concentration, non-turbulent parent current, approaching a viscoplastic behavior (Palladino and Valentine, 1995; Palladino and Simei, 2002). Noteworthy, in the WOB case, the inverse lateral grading of juvenile clasts holds not only for light pumice clasts (as previously reported for other examples; e.g. Palladino and Valentine, 1995), but also for high-density scoria clasts (1120-1400 kg/m^3). For comparison, the Pian di Rena pyroclastic flow unit of the Sovana eruption (Latera, Vulsini) contains coarse black scoria clasts very similar in texture and density to the WOB ones, yet they clearly show normal lateral grading parallel to coexisting lithics (Palladino and Valentine, 1995).

Concerning the thickness-distance trend (Figure 4), we observe a slightly increasing deposit thickness away from source in intermediate settings, where the pyroclastic current travelled essentially over an unconfined, slightly inclined topography, followed by a marked increase in thickness toward more distal settings, where the current advanced along radial topographic channels. In light of Giordano and Doronzo (2017) and Palladino and Giordano (2019), the observed AR$_t$-Lt pattern (i.e., steep positive gradient in Figure 5) implies that, while the current was depositing at each site, most of the pyroclastic material was transported ahead by the surviving current. This indicates a "forced" behavior of the WOB parent flow, which may either result from a sustained flow due to continuous feeding with high mass discharge rate at the source vent ("source forcing") and/or be favoured locally by steep slopes or topographic channels ("topographic forcing").

Typically, moderate- to large-volume pyroclastic currents derived from collapsing Plinian columns or caldera-forming eruptive phases may exhibit a forced regime on a regional scale (e.g., Pozzolane Rosse, Colli Albani; Cerro Galan Ignimbrite, Argentina; Giordano and Doronzo, 2017; ARL, Latera; Palladino and Giordano, 2019), which could be enhanced locally by topographic

effects. Coupled, opposite lithic and pumice clast size trends (expressed by CRl and CRp) downcurrent, in response to the density contrast with the "flow" medium of gas and fine particles, would be compatible with high particle concentration and non-turbulent flow regime (Palladino and Valentine, 1995). Specifically, in the WOB case, the inverse lateral grading of dense scoria clasts put a constraint to the minimum density of the transporting flow (i.e. >1120-1400 kg/m^3). Quite similar CR-L$_t$ trends have been reported for the ARL unit of Latera (Palladino and Giordano, 2019), although in the ARL case the increasing CRp was shown by highly vesicular, low-density (ca. 700 kg/m^3) pumice clasts. Thus, WOB represents an even more striking example approaching the high particle concentration, non-turbulent end-member of the classical spectrum of pyroclastic current dynamics.

We infer that the general tendency of increasing thickness with distance shown by the WOB main pyroclastic flow unit was essentially due to source forcing (sustained mass discharge rate) from proximal to intermediate settings, while advancing across a relatively open country. The source-driven forced regime was enhanced by topographic forcing due to channeling along ENE-oriented topographic lows (parallel to the radial flow path) in distal settings, thus producing an increase of the bulk density of the current. The negative density contrast with the transporting current and, possibly, the concomitant effects of kinematic sieving and dispersive pressure (e.g., Palladino, 1996), would explain the prolonged transport of coarse scoria clasts in the upper zones of a high concentration pyroclastic current, and their overall inverse lateral grading as far as the final runout.

The emplacement of a high density pyroclastic current at the whole flow scale shows analogy with a dry debris flow dominated by a granular flow regime, in terms of overall mobility and maximum runout in response to topography and flow volume (Hsü, 1989; Hayashi and Self, 1992). By analogy with the mobility of dry debris flows (Staron and Lajeunesse, 2009) and with a previous application to a dense pyroclastic current (ARL unit; Palladino and Giordano, 2019), flow transport is controlled by two contributions: i) a flow regime dominated by *sliding*, in which the runout depends on the internal angle of friction of the granular material and is independent of flow volume, and ii) a flow regime dominated by *spreading*, in which the runout is strongly dependent on volume. Moderate-to large-volume pyroclastic currents, sustained by high mass discharge rates at source (i.e., from collapsing Plinian columns or caldera-forming events), would show an increasing *spreading* component of transport, which reflects in additional runout. On these grounds, in the WOB case, the *sliding* component of transport prevailed from proximal to intermediate settings, accounting for the prevailing tendency of the pyroclastic current to transport than to deposit. Thus, a relatively thin (a few meters-thick) deposit originated, with normal lateral grading of lithics. On the other hand, the *spreading* component dominated further downcurrent, resulting in increasing pyroclast accumulation (up to tens of meters of thickness) as far as the final runout distance.

With respect to a spreading apron in an open country (as was the case of the previously documented ARL example), in the specific study case, the superposition of a forced regime induced by topographic channelling may have enhanced the mobility and final runout of distinct lobes of the pyroclastic current. Topographic forcing also enhanced the flow density and thus the capability to transport the coarsest scoria clasts as far as the most distal reaches. The maximum pyroclast accumulation eventually occurred toward the end of flow transport, which was dictated by the exhaustion of the forced flow regime (rather than by blocking due to topographic obstacles).

REFERENCES

Acocella V., Palladino D.M., Cioni R., Russo P., Simei S., 2012. Caldera structure, amount of collapse and erupted volumes: the case of Bolsena Caldera, Italy. Geological Society of America Bulletin 124, 1562-1576.

Andrews B.J. and Manga M., 2011. Effects of topography on pyroclastic density current runout and formation of coignimbrites. Geology 39, 1099-1102.

Bonadonna C., Cioni R., Costa A., Druitt T., Phillips J., Pioli L., Andronico D., Harris A., Scollo S., Bachmann O., Bagheri G., Biass S., Brogi F., Cashman K., Dominguez L., Dürig T., Galland O., Giordano G., Gudmundsson M., Hort M., Höskuldsson A., Houghton B., Komorowski J.C., Küppers U., Lacanna G., Le Pennec J.L., Macedonio G., Manga M., Manzella I., de' Michieli Vitturi M., Neri A., Pistolesi M., Polacci M., Ripepe M., Rossi E., Scheu B., Sulpizio R., Tripoli B., Valade S., Valentine G.A., Vidal C., Wallenstein N., 2016. MeMoVolc report on classification and dynamics of volcanic explosive eruptions. Bulletin of Volcanology 78, 84.

Branney M.J. and Kokelaar P., 2002. Pyroclastic density currents and the sedimentation of ignimbrites. Geological Society of London Memoirs 27, 1-143.

Capaccioni B. and Sarocchi D., 1996. Computer-assisted image analysis on clast shape fabric from the Orvieto-Bagnoregio ignimbrite (Vulsini District, central Italy): implications on the emplacement mechanisms. Journal of Volcanology and Geothermal Research 70, 75-90.

Dellino P., Zimanowski B., Büttner R., La Volpe L,, Mele D.,

Sulpizio R., 2007. Large-scale experiments on the mechanics of pyroclastic flows: Design, engineering, and first results. Journal of Geophysical Research-Solid Earth 112: B04202.

Doronzo D.M., 2012. Two new end members of pyroclastic density currents: Forced convection-dominated and inertia-dominated. Journal of Volcanology and Geothermal Research 219-220, 87-91.

Druitt T.H., 1998. Pyroclastic density currents. In: "The Physics of Explosive Volcanic Eruptions", Gilbert, J.S., Sparks, R.S.J. (Eds.), Geological Society London Special Publications 145, 145-182.

Dufek J., Wexler J., Manga M., 2009. Transport capacity of pyroclastic density currents: Experiments and models of substrate-flow interaction. Journal of Geophysical Research 114, B11203.

Fauria K.E., Manga M., Chamberlain M., 2016. Effect of particle entrainment on the runout of pyroclastic density currents. Journal of Geophysical Research-Solid Earth 121, 6445-6461.

Fisher R.V., Orsi G., Ort M., Heiken G., 1993. Mobility of a large-volume pyroclastic flow-emplacement of the Campanian Ignimbrite, Italy. Journal of Volcanology and Geothermal Research 56, 205-220.

Giordano G. and Doronzo D.M., 2017. Sedimentation and mobility of PDCs: a reappraisal of ignimbrites' aspect ratio. Scientific Reports 7, 4444.

Hayashi J.N. and Self S., 1992. A comparison of pyroclastic flow and debris avalanche mobility. Journal of Geophysical Research 97, 9063-9072.

Hsü K.J., 1989. Physical Principles of Sedimentology, Springer, Berlin, 234 pp.

Marra F., Costantini L., Di Buduo G.M., Florindo F., Jicha B., Monaco L., Palladino D.M., Sottili G., 2019. Combined glacio-eustatic forcing and volcano-tectonic uplift: geomorphological and geochronological constraints on the Tiber River terraces in the eastern Vulsini Volcanic District (central Italy). Global and Planetary Change 182, 103009, 12 pp.

Nappi G., Capaccioni B., Mattioli M., Mancini E., Valentini L., 1994. Plinian fall deposits from Vulsini Volcanic District (Central Italy). Bulletin of Volcanology 56, 502-515.

Nappi G., Renzulli A., Santi P., Gillot Y., 1995. Geological evolution and geochronology of the Vulsini volcanic district (central Italy). Bollettino della Società Geologica Italiana 114, 599-613.

Palladino D.M., 1996. Application of dimensional analysis technique to grading processes in pyroclastic flows. Periodico di Mineralogia 65, 15-20.

Palladino D.M., 2017. Simply pyroclastic currents. Bulletin of Volcanology 79, 53.

Palladino D.M., Gaeta M., Giaccio B., Sottili G., 2014. On the anatomy of magma chamber and caldera collapse: the example of trachy-phonolitic explosive eruptions of the Roman Province (central Italy). Journal of Volcanology and Geothermal Research 281, 12-26.

Palladino D.M. and Giordano G., 2019. On the mobility of pyroclastic currents in light of deposit thickness and clast size trends. Journal of Volcanology and Geothermal Research 384, 64-74.

Palladino D.M. and Simei S., 2002. Three types of pyroclastic currents and their deposits: examples from the Vulsini Volcanoes, Italy. Journal of Volcanology and Geothermal Research 116, 97-118.

Palladino D.M., Simei S., Sottili G., Trigila R., 2010. Integrated approach for the reconstruction of stratigraphy and geology of Quaternary volcanic terrains: an application to the Vulsini Volcanoes (central Italy). In: Stratigraphy and geology in volcanic areas. (Eds.): G. Groppelli and L. Viereck, Geological Society of America, Special Paper 464, 66-84.

Palladino D.M. and Valentine G.A., 1995. Coarse-tail vertical and lateral grading in pyroclastic flow deposits of the Latera Volcanic Complex (Vulsini, Central Italy): origin and implications for flow dynamics. Journal of Volcanology and Geothermal Research 69, 343-364.

Sparks R.S.J. and Walker G.P.L., 1977. The significance of vitric-enriched air-fall ashes associated with crystal-enriched ignimbrites. Journal of Volcanology and Geothermal Research 2, 329-341.

Sulpizio R., Dellino P., Doronzo D.M., Sarocchi D., 2014. Pyroclastic density currents: state of the art and perspectives. Journal of Volcanology and Geothermal Research 283, 36-65.

Staron L. and Lajeunesse E., 2009. Understanding how volume affects the mobility of dry debris flows. Geophysical Research Letters 36, L12402.

Valentine G.A., 1987. Stratified flow in pyroclastic surges. Bulletin of Volcanology 49, 616-630.

Valentine G.A., 1998. Damage to structures by pyroclastic flows and surges, inferred from nuclear weapons effects. Journal of Volcanology and Geothermal Research 87, 117-140.

Valentine G.A., Palladino D.M., DiemKaye K., Fletcher C., 2019. Lithic-rich and lithic-poor ignimbrites and their basal deposits: Sovana and Sorano eruptive units (Latera caldera, Italy). Bulletin of Volcanology 81, 29.

Walker G.P.L., 1983. Ignimbrite types and ignimbrite problems. Journal of Volcanology and Geothermal Research 17, 65-88.

Walker G.P.L., Heming R.F., Wilson C.J.N., 1980. Low aspect ratio ignimbrites. Nature 283, 286-287.